ACS APPLIED MATERIALS & INTERFACES

Research Article

www.acsami.org

Highly Transparent and Efficient Counter Electrode Using SiO_2/PEDOT−PSS Composite for Bifacial Dye-Sensitized Solar Cells

Dandan Song,[†] Meicheng Li,*[,†,‡] Yingfeng Li,[†] Xing Zhao,[†] Bing Jiang,[†] and Yongjian Jiang[†]

[†]State Key Laboratory of Alternate Electrical Power System with Renewable Energy Sources, School of Renewable Energy, North China Electric Power University, Beijing 102206, China

[‡]Suzhou Institute, North China Electric Power University, Suzhou 215123, China

Supporting Information

ABSTRACT: A highly transparent and efficient counter electrode was facilely fabricated using SiO_2/poly(3,4-ethylenedioxythiophene)-poly(styrenesulfonate) (PEDOT−PSS) inorganic/organic composite and used in bifacial dye-sensitized solar cells (DSCs). The optical properties of SiO_2/PEDOT−PSS electrode can be tailored by the blending amount of SiO_2 and film thickness, and the incorporation of SiO_2 in PEDOT−PSS provides better transmission in the long wavelength range. Meanwhile, the SiO_2/PEDOT−PSS counter electrode shows a better electrochemical catalytic activity than PEDOT−PSS electrode for triiodide reduction, and the role of SiO_2 in the catalytic process is investigated. The bifacial DSC with SiO_2/PEDOT−PSS counter electrode achieves a high power conversion efficiency (PCE) of 4.61% under rear-side irradiation, which is about 83% of that obtained under front-side irradiation. Furthermore, the PCE of bifacial DSC can be significantly increased by adding a reflector to achieve bifacial irradiation, which is 39% higher than that under conventional front-side irradiation.

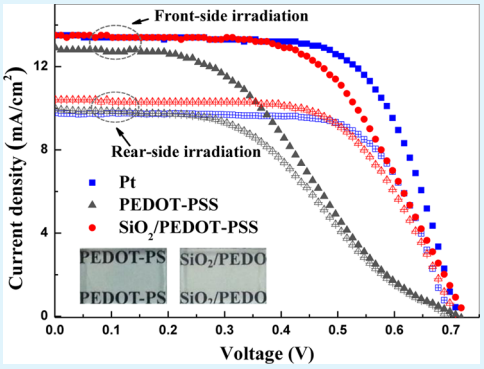

KEYWORDS: *bifacial dye sensitized solar cells, SiO_2/PEDOT−PSS inorganic/organic composite, counter electrode, transparent*

1. INTRODUCTION

Dye-sensitized solar cells (DSCs) have been rapidly developed in recent years for their potential advantages including cost-effective to fabricate and high energy conversion efficiency.[1−3] Fabricating DSCs with high efficiency and making the DSC systems more practical for commercial production are new challenges in the development of DSCs.[4] Bifacial DSCs, which are capable of converting incident sunlight to electricity at the front and rear faces of the cell, can produce up to 50% more electric power and can be used in a broaden filed.[5,6] A conventional DSC consists of a dye-sensitized TiO_2 photoanode, an iodide/triiodide (I^-/I_3^-) redox electrolyte and a counter electrode (CE). In bifacial DSC, a transparent CE is required. The most common CE used in DSC is the platinized FTO, which exhibits high catalytic activity for the reduction of I_3^- to I^-.[7] However, although a thin layer of Pt is transparent, it suffers from the high reflectance[8] and is not an ideal candidate for transparent CE in bifacial DSCs. Furthermore, Pt is scarce and thus is not suitable for large scale application. Therefore, the development of transparent and low-cost CE is of great importance in developing bifacial DSCs.

Although many low-cost materials, such as carbonaceous materials and metal compounds,[9−11] have been proposed as catalysts for CE in DSCs, these materials are usually dark and/or require a thick film to achieve a high catalytic activity,[4,9−11] which makes the CE nontransparent to visible light. Several kinds of optically transparent CE have been investigated, such as polyaniline,[12] polypyrrole,[13] and the PCE ratio (the ratio of PCE obtained from rear-side to that obtained from front-side irradiation) of the bifacial DSCs using these CEs are generally in the scale of 50−70%.[5,12,13] By improving the fabrication method, Zhao et al. reported a highly transparent carbon CE and got the highest PCE ratio of around 83.0%.[14] Until now, only limited materials have been reported to be suitable for CEs in bifacial DSCs, and the exploration of novel optically transparent and low-cost CE is crucial.

Poly(3,4-ethylenedioxythiophene) (PEDOT) is a highly conductive polymer and is soluble in water when doped with poly(styrenesulfonate) (PSS).[15] A thin layer of PEDOT (several tens of nanometers) is optical transparent and has the potential to be used as transparent CE for bifacial DSCs. As the raw materials of synthesizing PEDOT−PSS are abundant and the fabrication of PEDOT−PSS film is facile, the PEDOT based CEs are low-cost. In addition, solution-processed PEDOT-based CEs also enable the fabrication of flexible DSCs.[16] However, though a thick and porous layer of PEDOT performs a high catalytic activity towards triiodide reduction, the thin PEDOT−PSS film fabricated from its aqueous solution has poor performance as CE in DSCs. The incorporation of nanomaterials (such as graphene,[17] TiS_2[18]) in PEDOT−PSS

Received: January 5, 2014
Accepted: May 6, 2014
Published: May 6, 2014

can improve the catalytic activity, whereas the absorption of the nanomaterial induces a trade-off between the catalytic activity and the optical transparency, which results in low catalytic activity when the transparency is reasonable.

Therefore, in this work, we report a highly transparent and low-cost CE using silica (SiO_2) nanoparticles and poly(3,4-ethylenedioxythiophene)-poly(styrenesulfonate) (PEDOT−PSS) inorganic/organic composite, and applied it in bifacial DSCs. The SiO_2/PEDOT−PSS CE was fabricated by spin-coating technique from the aqueous solution of mechanical mixture of SiO_2 and PEDOT−PSS. The optical transparency and catalytic properties can be simultaneously improved with the incorporation of SiO_2 in PEDOT−PSS. The DSC with SiO_2/PEDOT−PSS CE performs a comparable PCE to the one with Pt CE and a high PCE ratio of 81−83% according to different blend amounts of SiO_2. The reasons for the high transparency and the high catalytic activity in SiO_2/PEDOT−PSS CE were investigated. Furthermore, we proved that the PCE of bifacial DSC with SiO_2/PEDOT−PSS CE could be significantly increased under bifacial irradiation. The high transparency, high catalytic activity, low-cost, and simple fabrication process highlight the the advantages and the potential application of SiO_2/PEDOT−PSS CE in commercial production of low-cost and effective bifacial DSCs.

2. RESULTS AND DISCUSSION

The bifacial cell shown in Figure 1 comprises a FTO glass coated with a dye-sensitized mesoporous TiO_2 photoanode, a

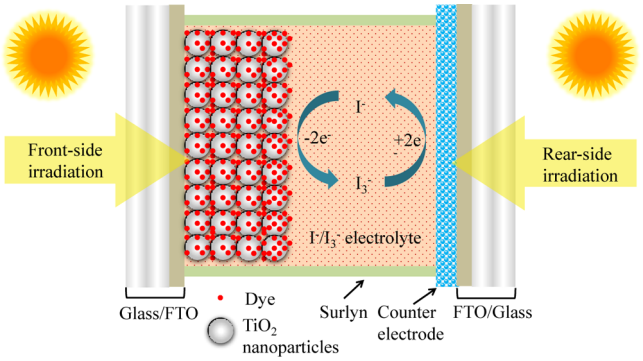

Figure 1. Schematic device structure of bifacial DSCs.

FTO glass coated with transparent CE, and the electrolyte filled in the space between the photoanode and CE. The bifacial cell can be irradiated through both photoanode side (front-side) and CE side (rear-side). In the case of front-side irradiation, the incident light are directly absorbed by the dye in photoanode; while in condition of rear-side irradiation, the incident light transmits through the CE and electrolyte, and is then absorbed by the dye in photoanode. Therefore, the transparency of the CE is important to achieve a reasonable photocurrent under the conditions of rear-side irradiation.

Figure 2a shows the UV−vis transmitted spectra of FTO glass, Pt CE, PEDOT−PSS and SiO_2/PEDOT−PSS (40 mg SiO_2 dispersed in 1 ml PEDOT−PSS aqueous solution) CEs, and the UV-vis absorption spectrum of N719 dye. The measurement was carried out using a spectrometer with an integrating sphere, taking into account diffuse transmittance. The FTO glass has a mean transmittance of 80% in the visible light region (350−800 nm). In the case of a 230 nm thick PEDOT−PSS layer (fabricated at a spin-coating speed of 1000 rpm) coated FTO glass, the transmittance is above 60% in the wavelength region of 350−600 nm. When using SiO_2/PEDOT−PSS coated on FTO glass fabricated under same conditions, the transmittance is about 70% over a wide wavelength range from 350 to 800 nm, indicating that the incorporation of SiO_2 in PEDOT−PSS can improve the transmittance, especially in the long wavelength region. For comparison, platinized FTO fabricated by thermo-decomposition of H_2PtCl_6 on FTO glass was also characterized, and it has a mean transmittance of 70% in the wavelength region of 550-800 nm and down to 55% at 380 nm. Considering the absorption of N719 dye that has two absorption peaks at 380 and 530 nm, respectively, PEDOT−PSS and SiO_2/PEDOT−PSS are more suitable for the use of transparent CEs than Pt CE.

As the film transmittance usually depends strongly on film thickness which can be varied by chaning the spin-coating speed in fabrication, so the investigation of the relation between film thickness and transmittance is necessary. It is found that the transmittance of PEDOT−PSS and SiO_2/PEDOT−PSS CEs can be further improved by decreasing the film thickness using high spin-coating speeds. As depicted in Figure 2b, the CEs prepared at a spin-coating speed of 5000 rpm show high transmittance above 70% in a wide wavelength range (350−800 nm). It can also be seen that SiO_2/PEDOT−PSS performs much better transmittance than PEDOT−PSS with similar thickness. Figure 2b inset shows the digital photographs of PEDOT−PSS and SiO_2/PEDOT−PSS CEs, from which it can be observed that these two CEs are highly transparent and

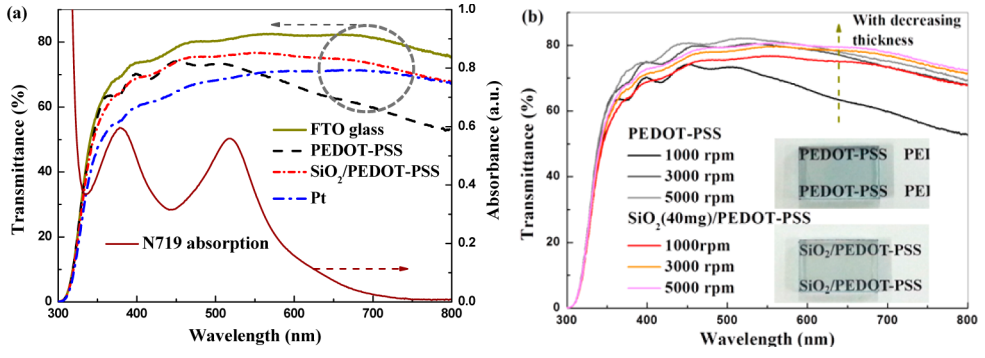

Figure 2. (a) Transmittance spectra of different electrodes and the absorption spectrum of N719 dye; (b) transmittance spectra of PEDOT−PSS and SiO_2/PEDOT−PSS CEs with different thicknesses. Inset: the digital photographs of PEDOT−PSS and SiO_2/PEDOT−PSS CEs fabricated at a speed of 5000 rpm.

dx.doi.org/10.1021/am500082x | ACS Appl. Mater. Interfaces 2014, 6, 7126−7132

SiO_2/PEDOT−PSS CE appears slightly scattering to the bare eye.

It is worth noting that the improvement in transmittance with SiO_2 is not simply due to the effect of thickness or PEDOT−PSS content, as a decrease in thickness or PEDOT−PSS content will increase the transmittance uniformly in the whole wavelength range, whereas with the doping of SiO_2 in PEDOT−PSS the increase in transmittance is more obvious at long wavelengths. The improved transmittance of the SiO_2/PEDOT−PSS layers is attributed to the change in the absorption property of PEDOT−PSS when SiO_2 is incorporated. PEDOT−PSS was found to be very anisotropic, uniaxial with the optic axis parallel to the surface normal.[19] As the absorption in the surface plane is especially higher in the long wavelength region (>400 nm), a decrease in anisotropy of PEDOT−PSS film leads to a more obvious decrease in absorption at long wavelengths. The anisotropy of PEDOT−PSS film is due to the orientation of the polymer chain along the film surface which may be caused by the high rate of spinning of the viscous solutions PEDOT−PSS. In SiO_2/PEDOT−PSS film, as the SiO_2 nanoparticles and PEDOT−PSS chains are homogeneous mixed, the interchain interactions of the PEDOT−PSS is decreased. Hence, the activation barrier for the reorientation of the polymer chains is also decreased, which causes a decrease in anisotropy of SiO_2/PEDOT−PSS film, leading to the lower absorption (higher transmittance) especially at long wavelengths.

These different transparent CEs were assembled together with a dye-sensitized TiO_2 mesoporous photoanode to fabricate bifacial DSCs. To get a reasonable efficiency in condition of front-side irradiation, the thickness of the photoanode is ∼12 μm, which is an optimized thickness for front-side irradiation. As photoexcitation in such a thick TiO_2 electrode occurs mostly around the side being irradiated according to Beer-Lambert Law, the electron path in TiO_2 conduction band is shorter in condition of front-side irradiation and the hole path is longer in comparison to those for the condition of rear-side irradiation, which reduces the differences in conversion efficiencies for front and rear irradiation.[5] Hence, the conversion efficiency for rear-side irradiation is also expected to be reasonable.

Figure 3 shows the photovoltaic parameters of short circuit current density (J_{SC}), open circuit voltage (V_{OC}), fill factor (FF) and power conversion efficiency (PCE) of DSCs using PEDOT−PSS and SiO_2/PEDOT−PSS CEs fabricated at different spin-coating speeds irradiated from front- and rear-side, respectively. The J_{SC} for all front-side irradiation condition is larger than that for the same condition with rear-side irradiation due to the absorption of counter electrode and I^-/I_3^- electrolyte.[5,20] With decreasing CE thickness (corresponding to higher spin-coating speed and higher transmittance), the J_{SC} in condition of rear-side irradiation gradually increases and achieves a highest J_{SC} ratio of 77.5% for PEDOT−PSS CE with a thickness of 50 nm and 80.0% for SiO_2/PEDOT−PSS CE with a thickness of 550 nm, respectively. The V_{OC} shows little change with decreasing CE thickness. The V_{OC} for any rear-side irradiation is lower than that for front-side irradiation, probably resulting from the increased carrier recombination in photoanode due to the longer electron path. With the reduction of CE thickness, the FF is lowered as a result of the decreased catalytic active area in thinner CE. The PCE of DSCs under front-side irradiation exhibits little change with the variation in CE thickness, while the PCE under rear-side irradiation gradually increases. Correspondingly, the PCE ratio also

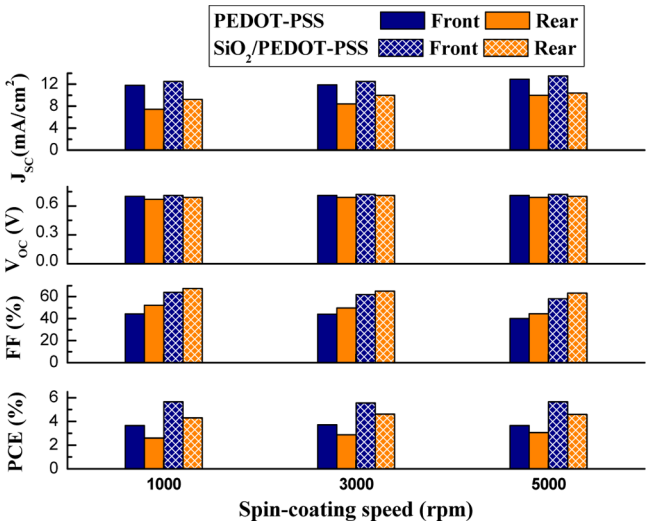

Figure 3. Photovoltaic parameters of DSCs with PEDOT−PSS or SiO_2/PEDOT−PSS CE fabricated at different spin-coating speeds, measured under illumination of 100 mW/cm^2 from front-side and rear-side, respectively.

increases from 71.0 to 83.6% for PEDOT−PSS CE. In DSC using SiO_2/PEDOT−PSS CE, the maximum PCE ratio is 82.9% with a CE thickness of 550 nm. From the photovoltaic results, it can also be seen that the J_{SC} ratio and PCE ratio for SiO_2/PEDOT−PSS CE prepared at 1000 rpm are both higher than those for PEDOT−PSS CE prepared under same conditions, proving that the increase of transmittance in a wide wavelength range is effective and important to obtain the high performance of bifacial DSCs.

Besides the optical effect, the introduction of SiO_2 in PEDOT−PSS also performs other effects. As can be seen from Figure 3, the FF is obviously higher in DSCs using SiO_2/PEDOT−PSS CEs under same fabrication and irradiation conditions or with similar thicknesses. A higher FF generally results from the higher catalytic activity of the CE, which can be investigated by electrochemical studies.

The electrochemical impedance spectroscopy (EIS) measurements were carried out to investigate the electrochemical characteristics of PEDOT−PSS and SiO_2/PEDOT−PSS CEs on symmetric cells fabricated with two identical electrodes. The Nyquist plots are shown in Figure 4a and the equivalent circuit is shown in Figure 4a inset. The high-frequency intercept at the real axis (Z') represents the series resistance (R_S). Three arcs can be seen in Nyquist plots, corresponding to the charge transfer resistance (R_{CT}) and the capacitance (CPE) at electrolyte/electrode interface (the left arc), the porous diffusion impedance (Z_{diff}) of redox sites in porous electrode (the middle arc), and the Nernst diffusion impedance (Z_N) of redox sites in electrolyte (the right arc).[21−23] The R_S, R_{CT}, and Z_{diff} for these two CEs were obtained by fitting the experimental spectra with the equivalent circuit (shown in Figure 4a inset) using Zview software, and the values are listed in Table 1. It can be seen that R_S of SiO_2/PEDOT−PSS CE is 4.4 Ω higher than that of PEDOT−PSS CE, resulting from the dielectric property of SiO_2 nanoparticles which decreases the conductivity of the CE. , The R_{CT} and Z_{diff} which associate with the electrochemical catalytic property of CEs are much lower in the case of SiO_2/PEDOT−PSS CE than PEDOT−PSS CE, i.e., 1.4 Ω and 9.2 Ω for the SiO_2/PEDOT−PSS CE, whereas 6.6 and 78.6 Ω for the PEDOT−PSS CE, respectively. Because the

dx.doi.org/10.1021/am500082x | ACS Appl. Mater. Interfaces 2014, 6, 7126−7132

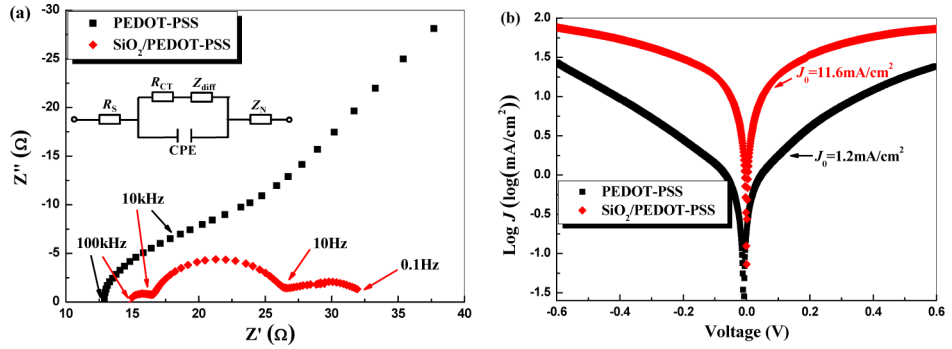

Figure 4. (a) Nyquist plots and (b)Tafel polarization curves of the symmetric cells with two identical CEs of PEDOT−PSS and SiO_2 (40 mg)/PEDOT−PSS, respectively.

Table 1. EIS Parameters of the Symmetric Cells with Two Identical CEs of PEDOT−PSS and SiO_2 (40 mg)/PEDOT−PSS, Respectively

counter electrodes	R_s (Ω)	R_{ct} (Ω)	Z_{diff} (Ω)
PEDOT−PSS	10.1	6.6	78.6
SiO_2/ PEDOT−PSS	14.5	1.4	9.2

R_{CT} varies inversely with the electrocatalytic activity for the reduction of I_3^-, the lower R_{CT} of SiO_2/PEDOT−PSS indicates that SiO_2/PEDOT−PSS CE has a better catalytic activity for I_3^- reduction than PEDOT−PSS. Besides, lower Z_{diff} corresponds to more efficient diffusion of I^-/I_3^- redox couple in the porous CE, which also facilities the reduction of I_3^-. Hence, it is reasonable that SiO_2/PEDOT−PSS CE possesses a better catalytic activity than PEDOT−PSS CE.

In addition, it can be found that though the impedance for PEDOT−PSS cell is large, the DSC using PEDOT−PSS CE shows reasonable device performance with similar J_{SC} and V_{OC} to the DSC using SiO_2/PEDOT−PSS CE. The J_{SC} is determined by the following equation

$$J_{SC} = J_{ph} - J_0\left[\exp\left(\frac{qAJ_{SC}R_{St}}{nKT}\right) - 1\right] - \frac{J_{SC}R_{St}}{R_{sh}}$$

where J_{SC} and J_0 are the generated photocurrent density and the saturation current density of the rectifying, respectively, A is the effective area of DSC, K is the Boltzmann constant, T is the absolute temperature, q is the electron charge, n is the ideal factor (for an ideal device, n = 1), R_{St} represents for the sum of the sheet resistance (sum of the R_s, charge transfer resistance at interfaces, diffusion impedance of redox couple, etc.), and R_{sh} is the shunt resistance. The value of R_{sh} can be estimated from the reciprocal of the slope of photocurrent-voltage curve at low voltages. The R_{sh} is sufficiently large in the DSC with either PEDOT:PSS or SiO_2/PEDOT:PSS CE as the slopes approximate to 0. The saturation current density J_0 determined from the dark current is much lower than the photocurrent. As a result, the change in the R_{St} plays shrunken effect on the J_{SC}. Hence, though the impedance for PEDOT−PSS cell is several times larger than that for SiO_2/PEDOT−PSS cell, the J_{SC} of the DSC using PEDOT−PSS CE is only a bit lower than that of the DSC using SiO_2/PEDOT−PSS CE. As V_{OC} is generally determined by the photoanode and meanwhile, the overpotential at the CE/electrolyte is low in the cases of these CEs, so the change in the CE has little effect on the V_{OC}.

Tafel polarization measurement is also a powerful method to characterize the electrochemical properties.[11,24] Figure 4b shows the Tafel plots of the symmetric cells similar to the one used in EIS measurements, which describes the dependence of electrical current density (J) on electrode potential. The exchange current (J_0), which is directly related to the catalytic activity of the electrode, can be calculated from the intersection of the linear anodic and cathodic curves.[11,24] The relationship between the J_0 and R_{CT} follows the equation below

$$J_0 = \frac{RT}{nFR_{CT}}$$

Where the R, T, F, and N are the gas constant, the temperature, the Faraday's constant, and the number of electrons involved in the reduction of I_3^- (n = 2), respectively.[14] In consistent with EIS results, J_0 is obviously higher in SiO_2/PEDOT−PSS CE (11.6 mA/cm^2) than in PEDOT−PSS CE (1.2 mA/cm^2), indicating that the catalytic activity of SiO_2/PEDOT−PSS is higher than that of PEDOT−PSS CE.

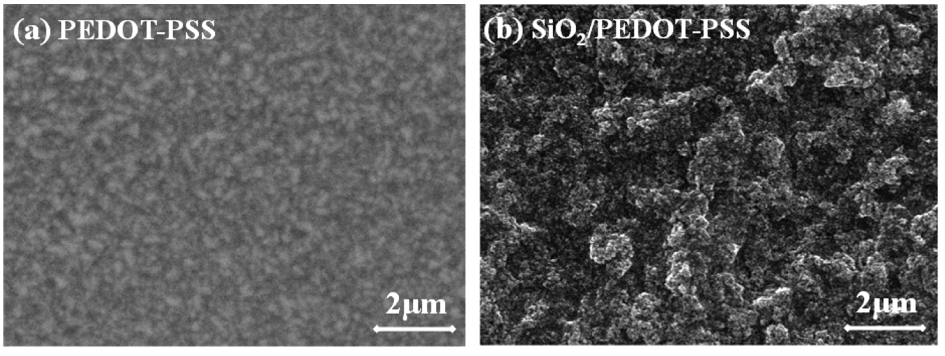

Figure 5. SEM images from (a) PEDOT−PSS film and (b) SiO_2 (40 mg)/PEDOT−PSS film.

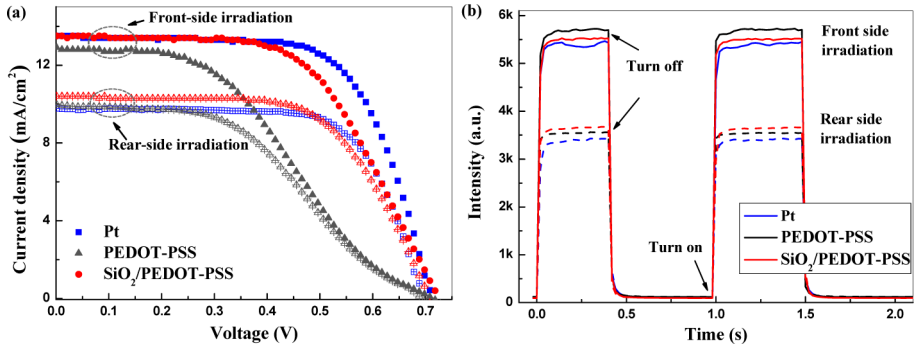

Figure 6. (a) Photocurrent density−voltage (J−V) curves and (b) stability of DSCs using different CEs under front-side and rear-side irradiation, respectively.

The EIS and Tafel results reveal that the incorporation of SiO_2 in PEDOT−PSS makes SiO_2/PEDOT−PSS CE to have superior electrochemical catalytic performance to PEDOT−PSS CE. However, SiO_2 on its own exhibits poor catalytic activity for I_3^- reduction, and thus introducing SiO_2 component in PEDOT−PSS has no positive effect on its catalytic activity. Therefore, the high catalytic activity in SiO_2/PEDOT−PSS CE probably results from the increased effective electrochemical catalytic surface area which can be studied by morphology study.[25,26] The surface morphologies of PEDOT−PSS and SiO_2/PEDOT−PSS CEs characterized by scanning electron microscopy (SEM) are shown in Figure 5. Figure 5a represents the top-view morphology of PEDOT−PSS coated FTO electrode, in which the rough texture is from FTO surface and the PEDOT−PSS layer is compactly formed on the FTO substrate. The mean surface roughness of PEDOT−PSS/FTO determined from atomic force microscope (AFM) topography image (see Figure S1a in the Supporting Information) is about 7.9 nm. In SiO_2/PEDOT−PSS coated FTO electrode (Figure 5b), the film is mesoporous with a lot of of interspaces and the particle-like SiO_2 are distributed homogeneously in PEDOT−PSS matrix. SiO_2/PEDOT−PSS electrode possesses a larger mean surface roughness (38.7 nm, obtained from AFM topography image shown in Figure S1b in the Supporting Information). The mesoporous feature of SiO_2/PEDOT−PSS electrode is caused by the high specifc surface area of SiO_2 nanoparticles (600 m^2/g). As a result, SiO_2/PEDOT−PSS film is expected to possess a larger electrochemical surface area than pristine PEDOT−PSS film, and meanwhile, the mesoporous feature also benefits the diffusion of redox sites, leading to the reduced R_{CT} and Z_{diff}. In addition, the homogeneous distribution of SiO_2 nanoparticles in PEDOT−PSS matrix enables the transport of generated holes from the reduction of I_3^- through the high conductive PEDOT−PSS chains, achieving good carrier transport in SiO_2/PEDOT−PSS CE.

For comparison, standard DSC using Pt CE was also fabricated, and it provides a PCE of 4.69% under rear-side irradiation and a PCE ratio of 73.5%, as shown in Figure 6a and Table 2. This PCE ratio is lower than that of DSC using PEDOT−PSS or SiO_2/PEDOT−PSS CE, in accordance with the low transmittance of Pt CE. Though the DSC using Pt CE still exhibits the highest FF thus the highest PCE under front-side irradiation, the performance of DSC using SiO_2/PEDOT−PSS CE can be further improved through the optimization of film thickness and amount of SiO_2. It is found that a thicker film leads to a higher FF (as shown in Figure 3 and Table S1 in the Supporting Information), and the variation of the amount of SiO_2 (0-60 mg) can lead to a change in FF from 44.3% to 63.9% (as shown in Figure S2 in the Supporting Information). Moreover, the catalytic activity and conductivity of PEDOT−PSS matrix in SiO_2/PEDOT−PSS CE can also be improved by referring to previous reports to get an ideal J_{SC}.[27,28] Hence, it can be speculated that SiO_2/PEDOT−PSS CE is potential to be as efficient as Pt CE.

Table 2. Photovoltaic Parameters of DSCs Using Different CEs under Front-Side and Rear-Side Irradiation, Respectively[a]

counter electrodes	irradiation side	J_{SC} (mA/cm^2)	V_{OC} (V)	FF (%)	PCE (%)	PCE ratio (%)
Pt	front	13.5	0.71	66.6	6.38	73.5
	rear	9.78	0.69	69.5	4.69	
PEDOT−PSS	front	12.9	0.71	40.0	3.66	83.6
	rear	9.98	0.69	44.4	3.06	
SiO_2/PEDOT−PSS	front	13.5	0.72	58.2	5.66	81.3
	rear	10.4	0.70	63.1	4.60	

[a]The PEDOT−PSS and SiO_2 (40 mg)/PEDOT−PSS were fabricated at a spin-coating speed of 5000 rpm.

The monochromatic incident photon-to-electron conversion efficiency (IPCE) spectra from DSCs employing different CEs have also been measured under front-side and rear-side irradiation, respectively. The IPCE ratio is relatively higher in DSC using PEDOT−PSS or SiO_2/PEDOT−PSS CE than that using Pt CE (as can be seen in Figure S3 in the Supporting Information), in accordance with the relative lower transmittance of Pt CE. It is also found that nearly all the incident light in short wavelength region (<450 nm) is totally absorbed by I^-/I_3^- electrolyte in all DSCs under rear-side irradiation, which weakens the transmittance advantage of PEDOT−PSS and SiO_2/PEDOT−PSS at short wavelengths. Therefore, employing an iodide-free electrolyte with less absorption, such as T^-/T_2 redox couple,[20] can further increase the PCE ratio of bifacial DSC with PEDOT−PSS or SiO_2/PEDOT−PSS CE. The stability of the DSCs using Pt, PEDOT−PSS, and SiO_2/PEDOT−PSS CE is investigated by recording the response intensity of photo-generated electron with or without the irradiation at 530 nm in condition of open circuit. As shown in Figure 6b, the intensity reaches a stable state in quite a short time (in 40 ms) after the irradiation is turn on in all DSCs under either front- or rear-side irradiation conditions. This demonstrates that the charge-carrier transport inside the cell is timely and effective, which implies that although the transport paths of electron and hole in condition of rear-side irradiation

are different from these in condition of front-side irradiation, they don't have much effect on the response time of the DSCs.

As the bifacial DSC can use the incident light from both faces, the photovoltaic performance of bifacial DSCs under bifacial irradiation have also been investigated. A white filter paper is used to act as a light reflector to reflect part of the incident light back to the DSC through the transparent electrodes, and the measured performance is shown in Figure 7.

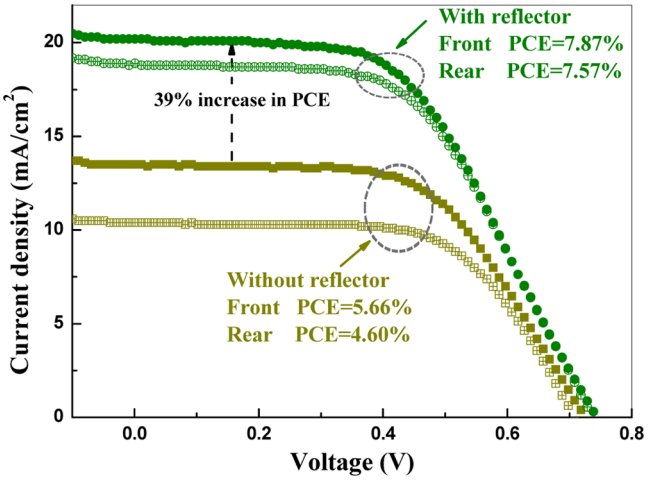

Figure 7. *J*–*V* curves of DSC using SiO_2 (40 mg) /PEDOT–PSS CE with or without paper reflector under front-side and rear-side irradiation, respectively.

The J_{SC} of the same DSC is significantly increased with the presence of reflector, and the PCE is also increased by almost 40%, demonstrating the high efficiency potential of bifacial DSCs.

3. EXPERIMENTAL SECTION

Preparation of CEs. SiO_2/PEDOT–PSS composites were prepared by dispersing commercially available SiO_2 nanoparticles (10-20 nm in diameter, purchased from DK nano) in PEDOT–PSS solution (Clevios PH1000), which was filtered with a 0.45 μm hydrophilic filter and doped with 6 vol % ethylene glycol before use, and then stirred and sonicated for several hours to form well dispersed solutions. The PEDOT–PSS-based CEs (SiO_2/PEDOT–PSS composites, pristine PEDOT–PSS) were fabricated by spin-coating of their solutions on ozone-treated FTO-glass followed by a drying process at 120 °C in air for 30 min. Pt electrode was fabricated by thermo-decomposition of H_2PtCl_6 isopropanol solution on ozone-treated FTO-glass at 450 °C in air for 20 min.

Fabrication of DSCs. TiO_2 film was prepared by doctor-blading of TiO_2 (P25 nanoparticles) slurry on $TiCl_4$ pre-treated FTO glass, followed by calcination at 500 °C in air for 30 min. After that, the TiO_2 film was post-treated in 40 mM $TiCl_4$ aqueous solution at 70 °C for 30 min and then calcinated at 500 °C in air for 30 min. After being cooled to 80 °C, the TiO_2 film was immersed in 0.3 mmol/L ethanol solution of N719 dye overnight. Then the dye-sensitized TiO_2 film was washed with anhydrous ethanol and dried. Finally, the dye-sensitized TiO_2 photoanodes and the as-fabricated CEs were assembled together with 60 μm thick Surlyn. The I^-/I_3^- liquid electrolyte with acetonitrile as the solvent was then injected between the two electrodes. The symmetric cell for the electrochemical measurements were fabricated by assembling two identical CEs together with 60 μm thick Surlyn and then injecting the electrolyte similar to the one used in fabricating DSCs.

Characterization. The transmitted spectra and absorption spectra were measured using a UV-vis spectrometer (Shimadzu UV2600) with an integrating sphere. The film thickness of the CEs were measured using a profiler (Bruker DektakXT). The morphology of the electrodes was characterized by scanning electron microscopy (FEI Quanta 200F) and atomic force microscope (Agilent 5500). The current density–voltage characteristics of DSCs were measured using a source meter (Keithley 2400) under AM 1.5G irradiation with a power density of 100 mW/cm^2 from a solar simulator (XES-301S+EL-100). The electrochemical impedance spectroscopy and Tafel polarization plots were carried out using the electrochemical workstation (CHI660D), performed on the symmetric cells. The frequency range varied from 100 kHz to 0.1 Hz. The monochromatic incident photon-to-electron conversion efficiency (IPCE) spectra and stability were characterized with a solar cell spectral response/QE/IPCE measurement system (Zolix SolarCellScan 100).

4. CONCLUSIONS

In conclusion, a novel counter electrode for bifacial DSCs was facilely constructed using SiO_2/PEDOT–PSS inorganic/organic composite. It is found that the incorporation of SiO_2 in PEDOT–PSS increases the transmittance in the long wavelength region and improves the catalytic activity for triiodide reduction due to the unique optical properties and large specific surface area of SiO_2 nanoparticles, respectively. Therefore, the counter electrode with SiO_2/PEDOT–PSS composite is highly transparent and catalytic activated. The bifacial DSC using SiO_2/PEDOT–PSS counter electrode exhibits a power conversion efficiency of 4.61% under rear-side irradiation, which is almost 83% of that under front-side irradiation. Furthermore, the PCE of bifacial DSC can be significantly increased by 39% by adding a reflector to achieve bifacial irradiation. Moreover, the PCE can be further improved by the further optimization of the blending amount of SiO_2, the film thickness and the annealing methods on PEDOT–PSS. The results obtained in this work reveal the advantages of SiO_2/PEDOT–PSS including ease of fabrication, low-cost, highly transparent and high catalytic activity for triiodide reduction, which provide new options for counter electrode materials in fabricating highly efficient bifacial DSCs.

■ ASSOCIATED CONTENT

Supporting Information

Figures S1–S3 and Table S1, in detail: Figure S1, AFM images from PEDOT–PSS film (a) and SiO_2 (40 mg)/PEDOT–PSS film (b). Figure S2, The photovoltaic parameters of DSCs using PEDOT–PSS based CEs with different SiO_2 doping amount, measured under illumination of AM 1.5G full sunlight (100 mW/cm^2) from front-side and rear-side, respectively. The CEs were fabricated at a spin-coating speed of 1000 rpm; Figure S3, The monochromatic incident photon-to-electron conversion efficiency (IPCE) spectra from DSCs employing different CEs measured under front-side and rear-side irradiation, respectively; Table S1, The photovoltaic parameters of DSCs with PEDOT–PSS or SiO_2 (40 mg)/ PEDOT–PSS CEs of different thicknesses under front-side and rear-side irradiation, respectively. This material is available free of charge via the Internet at http://pubs.acs.org/.

■ AUTHOR INFORMATION

Corresponding Author

*E-mail: mcli@ncepu.edu.cn. Tel: +86-10-61772951. Fax: +86-10-61772951.

Notes

The authors declare no competing financial interest.

■ ACKNOWLEDGMENTS

This work was supported partially by the National Natural Science Foundation of China (Grants 51372082, 51172069, 50972032, 61204064, 51202067, and 91333122), Ph.D. Programs Foundation of Ministry of Education of China (Grants 20110036110006, 20120036120006, 20130036110012), and the Fundamental Research Funds for the Central Universities.

■ REFERENCES

(1) Grätzel, M. Recent Advances in Sensitized Mesoscopic Solar Cells. *Acc. Chem. Res.* **2009**, *42*, 1788−1798.
(2) Hardin, B.E.; Snaith, H.J.; McGehee, M.D. The Renaissance of Dye-Sensitized Solar Cells. *Nat. Photonics* **2012**, *6*, 162−169.
(3) Hou, Y.; Wang, D.; Yang, X.H.; Fang, W.Q.; Zhang, B.; Wang, H.F.; Lu, G.Z.; Hu, P.; Zhao, H.J.; Yang, H.G. Rational Screening Low-Cost Counter Electrodes for Dye-Sensitized Solar Cells. *Nat. Commun.* **2013**, *4*, 1583.
(4) Fu, N. Q.; Fang, Y. Y.; Duan, Y. D.; Zhou, X. W.; Xiao, X. R.; Lin, Yo. High-Performance Plastic Platinized Counter Electrode via Photoplatinization Technique for Flexible Dye-Sensitized Solar Cells. *ACS Nano* **2012**, *6* (11), 9596−9605.
(5) Ito, S.; Zakeeruddin, S. M.; Comte, P.; Liska, P.; Kuang, D.; Grätzel, M. Bifacial Dye-Sensitized Solar Cells Based on an Ionic Liquid Electrolyte. *Nat. Photonics* **2008**, *2* (11), 693−698.
(6) Hubner, A.; Aberle, A. G.; Hezel, R. Novel Cost-Effective Bifacial Silicon Solar Cells with 19.4% Front and 18.1% Rear Efficiency. *Appl. Phys. Lett.* **1997**, *70* (8), 1008−1010.
(7) Lindström, H.; Holmberg, A.; Magnusson, E.; Lindquist, S. E.; Malmqvist, L.; Hagfeldt, A. A New Method for Manufacturing Nanostructured Electrodes on Plastic Substrates. *Nano Lett.* **2001**, *1* (2), 97−100.
(8) Mor, G. K.; Shankar, K.; Paulose, M.; Varghese, O. K.; Grimes, C. A. Use of Highly-Ordered TiO_2 Nanotube Arrays in Dye-Sensitized Solar Cells. *Nano Lett.* **2006**, *6* (2), 215−218.
(9) Huang, Z.; Liu, X.; Li, K.; Li, D.; Luo, Y.; Li, H.; Song, W.; Chen, L.; Meng, Q. Application of Carbon Materials as Counter Electrodes of Dye-Sensitized Solar Cells. *Electrochem. Commun.* **2007**, *9*, 596−598.
(10) Wu, M.; Lin, X.; Wang, Y.; Wang, L.; Guo, W.; Qi, D.; Peng, X.; Hagfeldt, A.; Grätzel, M. Economical Pt-Free Catalysts for Counter Electrodes of Dye-Sensitized Solar Cells. *J. Am. Chem. Soc.* **2012**, *134*, 3419−3428.
(11) Kung, C.W.; Chen, H.W.; Lin, C.Y.; Huang, K.C.; Vittal, R.; Ho, K.C. CoS Acicular Nanorod Arrays for the Counter Electrode of an Efficient Dye-Sensitized Solar Cell. *ACS Nano* **2012**, *6*, 7016−7025.
(12) Tai, Q.; Chen, B.; Guo, F.; Xu, S.; Hu, H.; Sebo, B.; Zhao, X. Z. In Situ Prepared Transparent Polyaniline Electrode and Its Application in Bifacial Dye-Sensitized Solar Cells. *ACS Nano* **2011**, *5* (5), 3795−3799.
(13) Bu, C.; Tai, Q.; Liu, Y.; Guo, S.; Zhao, X. A Transparent and Stable Polypyrrole Counter Electrode for Dye-Sensitized Solar Cell. *J. Power Sources* **2013**, *221*, 78−83.
(14) Bu, C.; Liu, Y.; Yu, Z.; You, S.; Huang, N.; Liang, L.; Zhao, X. Z. Highly Transparent Carbon Counter Electrode Prepared via an in Situ Carbonization Method for Bifacial Dye-Sensitized Solar Cells. *ACS Appl. Mater. Interfaces* **2013**, *5* (15), 7432−7438.
(15) Chen, J.G.; Wei, H. Y.; Ho, K. C. Using Modified Poly(3,4-ethylene dioxythiophene): Poly(styrene sulfonate) Film as a Counter Electrode in Dye-Sensitized Solar Cells. *Sol. Energy Mater. Sol. Cells* **2007**, *91*, 1472−1477.
(16) Lee, K. S.; Lee, Y.; Lee, J. Y.; Ahn, J.-H.; Park, J. H. Flexible and Platinum-Free Dye-Sensitized Solar Cells with Conducting-Polymer-Coated Graphene Counter Electrodes. *ChemSusChem* **2012**, *5*, 379−382.
(17) Hong, W.; Xu, Y.; Lu, G.; Li, C.; Shi, G. Transparent Graphene/PEDOT−PSS Composite Films as Counter Electrodes of Dye-Sensitized Solar Cells. *Electrochem. Commun.* **2008**, *10*, 1555−1558.
(18) Li, C.-T.; Lee, C.-P.; Li, Y.-Y.; Yeh, M.-H.; Ho, K.-C. A Composite Film of TiS_2/PEDOT:PSS as the Electrocatalyst for the Counter Electrode in Dye-Sensitized Solar Cells. *J. Mater. Chem. A* **2013**, *1*, 14888−14896.
(19) Pettersson, L. A.A.; Ghosh, S.; Inganäs, O. Optical Anisotropy in Thin Films of Poly(3,4-ethylenedioxythiophene)−Poly(4-styrenesulfonate). *Org. Electron.* **2002**, *3*, 143−148.
(20) Li, X.; Ku, Z.; Rong, Y.; Liu, G.; Liu, L.; Liu, T.; Han, H. Design of an Organic Redox Mediator and Optimization of an Organic Counter Electrode for Efficient Transparent Bifacial Dye-Sensitized Solar Cells. *Phys. Chem. Chem. Phys.* **2012**, *14* (41), 14383−14390.
(21) Xu, H.; Zhang, X.; Zhang, C.; Liu, Z.; Zhou, X.; Pang, S.; Chen, X.; Dong, S.; Zhang, Z.; Zhang, L.; Han, P.; Wang, X.; Cui, G. Nanostructured Titanium Nitride/PEDOT: PSS Composite Films as Counter Electrodes of Dye-Sensitized Solar Cells. *ACS Appl. Mater. Interfaces* **2012**, *4*, 1087−1092.
(22) Song, J.; Li, G. R.; Xiong, F. Y.; Gao, X. P. Synergistic Effect of Molybdenum Nitride and Carbon Nanotubes on Electrocatalysis for Dye-Sensitized Solar Cells. *J. Mater. Chem.* **2012**, *22*, 20580.
(23) Wang, Q.; Moser, J. E.; Grätzel, M. Electrochemical Impedance Spectroscopic Analysis of Dye-Sensitized Solar Cells. *J. Phys. Chem. B* **2005**, *109*, 14945−14953.
(24) Bard, A. J.; Faulkner, L. R. *Electrochemical Methods: Fundamentals and Applications*, 2nd ed.; John Wiley & Sons: New York, 2000; pp 103−104.
(25) Xia, J.; Masaki, N.; Jiang, K.; Yanagida, S. The Influence of Doping Ions on Poly (3, 4-ethylenedioxythiophene) as a Counter Electrode of a Dye-Sensitized Solar Cell. *J. Mater. Chem.* **2007**, *17*, 2845−2850.
(26) Song, D.; Li, M.; Bai, F.; Li, Y.; Jiang, Y.; Jiang, B. Silicon Nanoparticles/PEDOT−PSS Nanocomposite as an Efficient Counter Electrode for Dye-Sensitized Solar Cells *Funct. Mater. Lett.* **2013**, *6* (4), 1350048.
(27) Chiang, C.H.; Wu, C.G. High-Efficient Dye-Sensitized Solar Cell Based on Highly Conducting and Thermally Stable PEDOT:PSS/Glass Counter Electrode. *Org. Electron.* **2013**, *14*, 1769−1776.
(28) Ouyang, J.Y. Solution-Processed PEDOT:PSS Films with Conductivities as Indium Tin Oxide through a Treatment with Mild and Weak Organic Acids. *ACS Appl. Mater. Interfaces* **2013**, *5* (24), 13082−13088.